Magnetic properties of $CeSb_{1-x}Te_x$ solid solutions

D. Ravot
Equipe de Chimie Mettallurgique, Centre National de la Recherche Scientifique, 1 place A. Briand, F-92190 Meudon, France

A. Mauger
Department of Physics, University of California, Irvine, California 92717

J. C. Achard and M. Bartholin
Equipe de Chimie Metallurgique, Centre National de la Recherche Scientifique, 1 place A. Briand, F-92190 Meudon, France and Université de Toulon, F-83130 La Garde, France

J. Rossat Mignod
Centre d'Etude Nucléaire de Grenoble, 85X, F-38041 Grenoble Cedex, France
(Received 25 March 1983)

We report magnetic properties of $CeSb_{1-x}Te_x$ solid solutions in the whole range of composition $0<x<1$. We find that a simple Heisenberg interaction treated in the molecular-field approximation is sufficient to describe the experimental results at $x>0.05$. In particular, a linear x dependence of the effective exchange-coupling constants $\bar{\Gamma}_1$ and $\bar{\Gamma}_2$ between nearest and next-nearest neighbors, respectively, accounts for the nonlinear behavior of the variations of the Néel temperature $T_N(x)$ which goes through a minimum at $x\simeq 0.07$. This model, however, is too crude to account for the magnetic properties at concentrations $x<0.05$, such as a maximum of the crystal-field splitting energy $\Delta(x)$ between the Γ_7 and Γ_8 levels of the $4f$-electron states at $x\simeq 0.04$, a maximum of the paramagnetic Curie temperature $\Theta^*(x)$ at $x\simeq 0.02$, and a very strong monotonic decrease of $T_N(x)$ in the whole range $0<x<0.05$. To account for these experimental data, we have studied the fourth-order indirect exchange in the mixing parameter, derived after a canonical transformation of the Schrieffer-Wolff type is applied to the multisite Anderson model when both the crystal-field effects and the large spin-orbit coupling of the intermediate state of the Ce electron in the $4f$ subshell are taken into account. This model provides an overall understanding of the magnetic properties of $CeSb_{1-x}Te_x$ solutions at all x. A detailed discussion of this model with respect to previous models is also reported.

I. INTRODUCTION

Investigations of CeSb have revealed the very complicated magnetic phase diagram[1] due to strong anisotropic exchange interactions. This material crystallizes in the NaCl structure, and under the effect of the crystal field, the ${}^2F_{J=5/2}$ multiplet of the Ce^{3+} ion is split in a doublet Γ_7 and a quartet Γ_8 separated by an energy Δ. One peculiarity of CeSb is that the strength of the exchange interactions as measured by the Néel temperature $T_N=16$ K, has the same order of magnitude as the crystal-field energy $\Delta\simeq 28$ K.[2,3] To investigate the effects resulting from this feature, we have explored physical properties of $CeSb_{1-x}Te_x$ solid solutions. The Néel temperature of CeTe is much smaller, namely $T_N=2$ K,[4,5] although the parameter Δ is roughly the same as in CeSb.[5] Also the easy axis of magnetization is $\langle 100\rangle$ in CeSb and $\langle 111\rangle$ in CeTe. We can then infer that the mixing of CeTe and CeSb will lead to significant variations of both the anisotropy and strength of the magnetic interactions. Both transport[6] and magnetic measurements[7] have already revealed a nonlinear variation of Δ with x in such compounds, for small Te concentrations. In this paper, we try to reveal the nature of the microscopic anisotropic exchange interaction from the analysis of some magnetic properties in $CeSb_{1-x}Te_x$ in the whole range $0<x<1$.

In Sec. II we report measurements of the magnetic susceptibility at high temperature, together with the variations of the Néel temperature T_N as a function of x. In Sec. III these data are analyzed in the framework of various models assuming that the magnetic exchange is isotropic. It is shown that a two-parameter Heisenberg model is sufficient to reproduce most of the experimental properties in the range $0.05<x<0.7$, provided that crystal-field effects are taken into account. At higher concentrations, the Ruderman-Kittel-Kasuya-Yosida (RKKY) interaction accounts for the magnetic properties. The isotropic exchange models, however, fail to account for the magnetic properties in the range $0<x<0.05$. At such concentrations, the anisotropy of the indirect magnetic interaction between Ce ions plays an important role. Anisotropic exchange models are reviewed in Sec. IV. It is shown in particular, that the Anderson model is a suitable basis to analyze the deviation of the magnetic properties of the solid solutions with respect to the isotropic models.

II. EXPERIMENTS

The magnetic susceptibility χ has been measured as a function of the temperature T at various tellurium con-

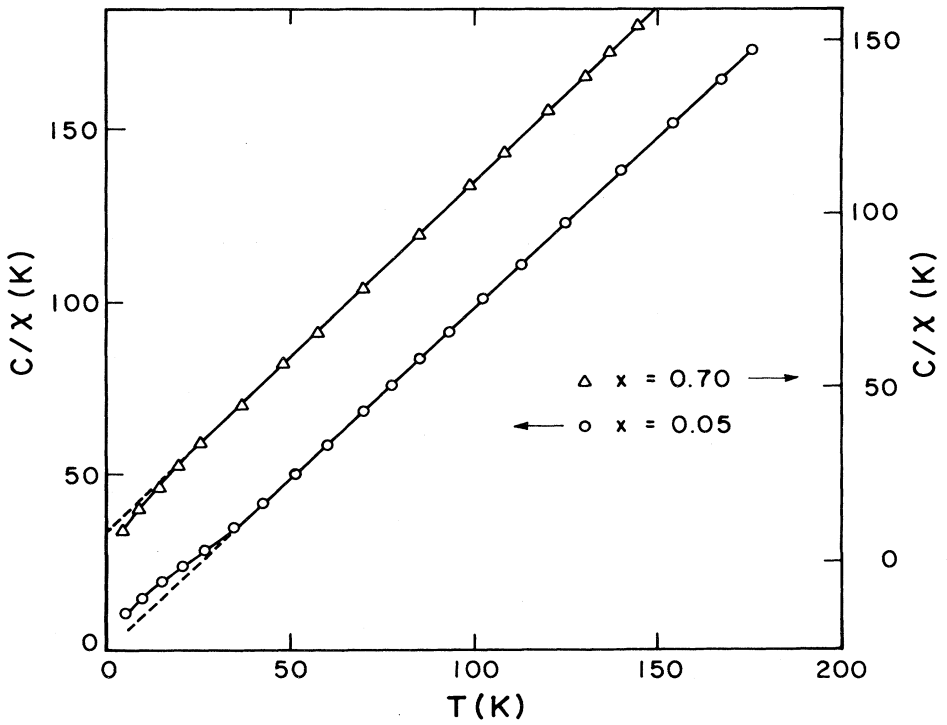

FIG. 1. Thermal variations of C/x, where C is the Curie constant and x the magnetic susceptibility, in $CeSb_{1-x}Te_x$, for $x=0.05$ and $x=0.70$. The broken line is the fit by a Curie-Weiss law, and the solid curve is the theoretical fit by Eqs. (7) or (11). The fact that the experimental value of C/x for $x=0.70$ at low temperatures is smaller than the value predicted by the Curie-Weiss law comes from the fact that the energy $E(\Gamma_8)-E(\Gamma_7)=\Delta$ is negative. To the contrary the large values of C/x for $x=0.05$ are associated with the fact that $\Delta>0$ at this Te concentration.

centrations x. The results for $x<0.05$ have been reported elsewhere.[7] At higher concentrations a single minimum of the curves $\chi^{-1}(T)$ is observed at the Néel temperature T_N. The results are illustrated in Fig. 1 for two different concentrations. In the range $T>4.2$ K the experimental data were obtained with the use of a magnetic balance in Laboratoire de Physique des Solides in Bellevue, and at $T<4.2$ K, $\chi(T)$ was measured with the use of the mutual inductance technique at Institut d'Electronique Fondamentale of the University of Orsay. The accuracy of the determination of T_N thus depends on which apparatus has been used, and is basically $\Delta T_N=\pm0.1$ K when $T_N<4.2$ K and $\Delta T_N=\pm0.3$ K when $T_N>4.2$ K. $\Delta T_N=\pm1$ K for $x=0.03$ because the value of T_N deduced from neutron experiments and from the susceptibility data on two different samples from the same bath

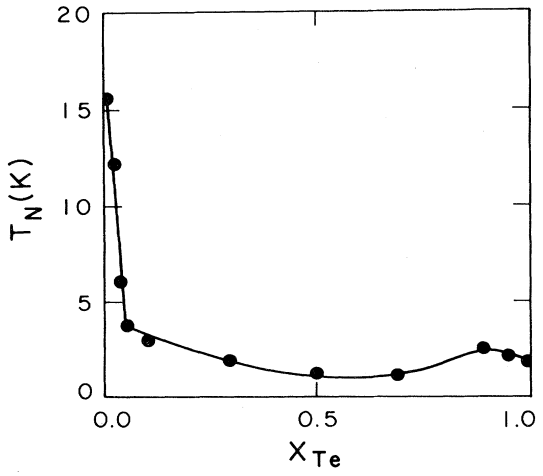

FIG. 2. Néel temperature T_N as a function of composition x in solid solutions $CeSb_{1-x}Te_x$.

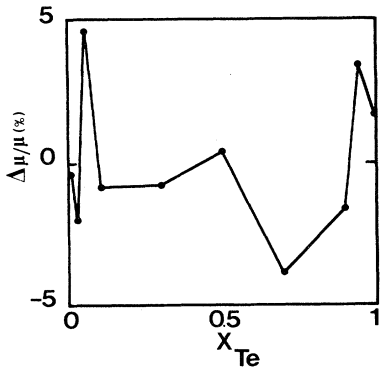

FIG. 3. Relative variations of the effective moment of the cerium ions with respect to the theoretical value $2.54\mu_B$, as a function of x in $CeSb_{1-x}Te_x$.

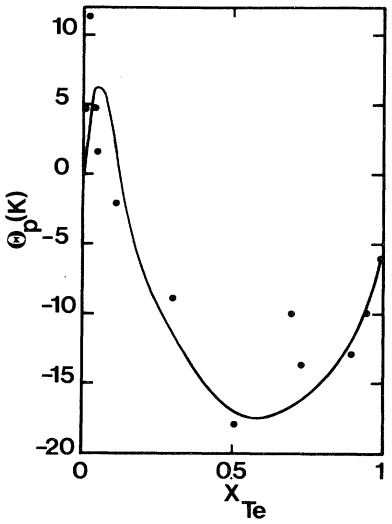

FIG. 4. Variations of the paramagnetic Curie temperature as a function of x. Experimental points $\Theta^*(x)$ are deduced from a Curie-Weiss law fitted at high temperature. The solid curve represents the theoretical variations $\Theta(x)$ in the RKKY model, for a ratio α/d, defined in Eq. (18), equal to 1.5.

differ by one degree. This can be understood by considering the variations of T_N as a function of x in $CeSb_{1-x}Te_x$ reported in Fig. 2. At small concentrations $x<0.05$, a very strong decrease of T_N with x is observed since T_N is reduced to 3.75 K in $CeSb_{0.95}Te_{0.05}$, to be compared with 16 K in CeSb. In particular, a difference of composition $\delta x=0.005$ at $x=0.03$ is sufficient to shift T_N by an amount of one degree. We can then infer that the uncertainty ΔT_N for this concentration x is dominated by uncertainty in the determination of x and in the homogeneity of the sample. At higher concentrations the variations $T_N(x)$ are much smaller and the uncertainty ΔT_N is due to the accuracy with which the temperature is measured in the experiments. T_N goes through a minimum at $x=0.7$ ($T_N=1.30$ K), then a secondary maximum ($T_N=2.60$ K) is observed for $x=0.90$.

At higher temperature $150<T<300$ K, the experimental curve $\chi^{-1}(T)$ has been fitted by the linear law,

$$\chi^{-1}=\frac{1}{C^*}(T-\Theta^*)\ , \tag{1}$$

using a least-squares method, for each concentration x investigated. Equation (1) is the usual Curie-Weiss law in a molecular-field approximation. Let r^2 be the determination coefficient of the linear regression. For all concentrations we found $1-r^2<10^{-2}$ so that Eq. (1) is well satisfied. The two regression coefficients C^* and Θ^* coincide with the Curie constant C and the paramagnetic Curie temperature Θ only in the limit $T\to\infty$. Such a limit, however, was not achieved in our experiments, because at room temperature, the thermal energy k_BT is not large compared with the crystal-field energy. We shall see, however, in Sec. III, that crystal-field effects do not affect significantly the slope C^{*-1} of the curves $\chi^{-1}(T)$, since $(C^*-C)/C<4\%$. We shall neglect this difference, and write $C^*\sim C$. From this Curie constant, we can derive the effective moment of the cerium ions. The results are reported in Fig. 3. For all concentrations x, we find values which are equal to the theoretical value $g\mu_B\sqrt{J(J+1)}=2.54\mu_B$, within 5%. The reasons why the crystal-field splitting affects significantly the values of Θ^* rather than the parameter C^{-1} will be reported in Sec. III, together with an estimation of $\Theta^*-\Theta$: The variation of Θ^* as a function of x are reported in Fig. 4. The uncertainty in the determination of Θ^* is large, because the deviation of the experimental curve $\chi^{-1}(T)$ from the linear behavior below 150 K restricts the range of temperature useful for the calculation of Θ^*. This range of temperature is not only narrow but also far from the values of Θ^* which result from the extrapolation of the Eq. (1) down to $T\sim\Theta^*\sim0$ K. To get an estimation on the accuracy of the determination of Θ^*, we have calculated the regression coefficients in the least-squares fit of $\chi^{-1}(T)$ by Eq. (1) in three ranges of temperatures: $150<T<200$ K, $150<T<250$ K, and $150<T<300$ K. In all cases $1-r^2$ was smaller than 10^{-2} and the variations of C were restricted to 1%; the variation of Θ^*, however, could reach 5 K. An illustration is given in Table I. We can then conclude that the uncertainty on Θ^* is typically $\Delta\Theta^*\sim5$ K. The experimental data in Fig. 4 shows that $\Delta\Theta^*(x)$ goes through a maximum at $x=0.02\pm0.01$ and a minimum at $x=0.55\pm0.05$. It is also likely that the curve $\Theta^*(x)$ shows a secondary maximum at $x=0.7$, but taking into account the value of $\Delta\Theta^*$, this superstructure needs to be confirmed by additional experiments in this range of tellurium concentrations.

TABLE I. Determination of the effective magnetic moment μ of Ce ions and effective paramagnetic Curie temperature Θ^* deduced from the least-squares fit of the magnetic susceptibility by a Curie-Weiss law at different ranges of temperature, for $x=0.035$.

Temperature range (K)	μ (μ_B)	Θ^* (K)
300–250	2.59	−1.93
300–200	2.56	+3.94
300–150	2.56	+4.67

III. ISOTROPIC EXCHANGE MODEL

Neutron experiments have revealed the existence of complex magnetic ordering in $CeSb_{1-x}Te_x$ up to $x\simeq0.02$,[8] which evidences highly anisotropic exchange interactions. For $x=0.035$ and $x=0.05$, however, such experiments have shown that the samples are simple type-I antiferromagnets (AF).[8] In the same way, the behavior of $\chi(T)$ for $x>0.035$ is characteristic of simple antiferromagnets with a single peak of magnetic susceptibility at the Néel temperature. Therefore, we are led to make the assumption that the substitution of Sb by Te by an amount $x>0.03$ anneals most of the anisotropy in $CeSb_{1-x}Te_x$. Hence, the exchange interactions should be related to the isotropic Heisenberg exchange operator,

$$\mathcal{H}_e=-\sum_{i,j}\Gamma_{ij}\vec{J}_i\cdot\vec{J}_j=-2\sum_{r=1}^{\infty}\Gamma_r\sum_{j=1}^{z_r}\vec{J}_i\cdot\vec{J}_j\ . \tag{2}$$

In the following, we study two magnetic properties of the solid solutions $CeSb_{1-x}Te_x$ with $0.05 \leq x \leq 1$ in the framework of this Hamiltonian treated in the molecular-field approximation. We preferred to choose $x=0.05$ rather than $x=0.035$ as the reference concentration because the uncertainty ΔT_N on the determination of the Néel temperature was larger for $x=0.035$ as above mentioned.

In Eq. (2) the factor $(g-1)^2$ where g is the Landé factor, arising from the Wigner-Eckart theorem has been included in the definition of the exchange integrals. We found it convenient to consider the sum over equivalent pair interactions between a given angular momentum $\vec{J}_i$ and the z_r spins of its rth neighbor shell characterized by the exchange integrals Γ_r.

A. Two-parameter model

The two-parameter approximation consists in replacing Eq. (2) by the effective Hamiltonian,

$$\mathcal{H}' = -2 \sum_{r=1}^{2} \overline{\Gamma}_r \sum_{j=1}^{z_r} \vec{J}_i \cdot \vec{J}_j \ . \tag{3}$$

Γ_1 and Γ_2 are the exchange integrals with the $z_1=12$ nearest (NN) and the $z_2=6$ next-nearest (NNN) neighbors of the Ce^{3+} ions, respectively. If $\overline{\Gamma}_{1,2}=\Gamma_{1,2}$, Eq. (3) is the truncation of the Heisenberg Hamiltonian to the NNN interactions. However, the magnetic interactions extend further out in the fcc lattice. This can be implicitly taken into account by allowing the effective exchange integrals $\overline{\Gamma}_1$ and $\overline{\Gamma}_2$ to be very different from the individual Γ_1 and Γ_2, as in europium chalcogenides, for example.[9] Γ_1 and Γ_2 in Eq. (3) then represent partial sums over exchange contributions projected into NN and NNN interactions alone. Equation (3) has been solved in the molecular-field approximation.[10] Depending on the values of $\overline{\Gamma}_1$ and $\overline{\Gamma}_2$, four different magnetic structures are possible in the fcc lattice. They are characterized by their $\vec{k}$ vector which is $k=(0,0,0)$ for the ferromagnetic ordering, and $k=(1,0,0)$, $k=(\frac{1}{2},\frac{1}{2},\frac{1}{2})$, $k=(1,\frac{1}{2},0)$ for the type-I, -II, -III antiferromagnetic ordering, respectively. In the whole text $\vec{k}$ vectors are expressed in $2\pi/a$ units, where a is the lattice parameter. These phases denoted, respectively, F, AF1, AF2, and AF3, are illustrated in Fig. 5.[10] The ordering temperature is proportional to the Fourier transform of $\overline{\Gamma}$: $T_{C,N}=C'\overline{\Gamma}(k)$ which reads, for the various phases,

$$\begin{aligned} &\text{AF1:}\ T_N=-2C'(2\overline{\Gamma}_1-3\overline{\Gamma}_2)\ , \\ &\text{AF2:}\ T_N=-6C'\overline{\Gamma}_2\ , \\ &\text{AF3:}\ T_N=2C'(\overline{\Gamma}_2-2\overline{\Gamma}_1)\ , \\ &F:\ T_C=\Theta\ . \end{aligned} \tag{4}$$

In all phases the paramagnetic Curie temperature Θ is given by

$$\Theta=6C'(2\overline{\Gamma}_1+\overline{\Gamma}_2) \tag{5}$$

The constant C' is defined by

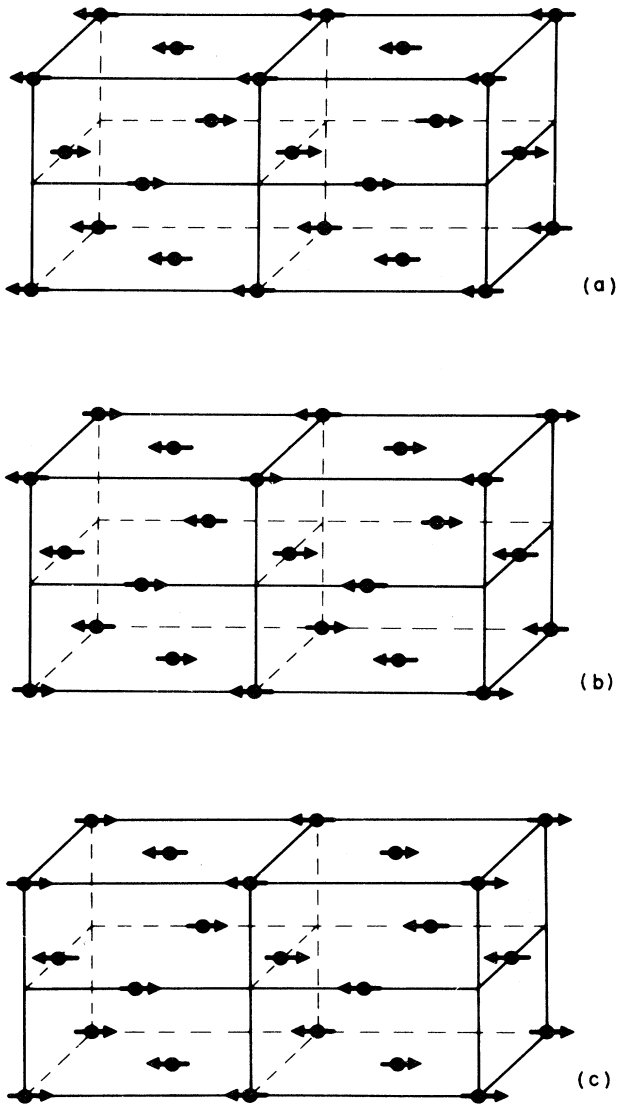

FIG. 5. (a) First, (b) second, and (c) third kind of antiferromagnetic ordering in the fcc lattice, named AF1, AF2, and AF3, respectively, in the text, from Ref. 10.

$$C'=\frac{2J(J+1)}{3k_B}\ . \tag{6}$$

The kind of magnetic ordering which actually occurs for a given $\overline{\Gamma}_1$ and $\overline{\Gamma}_2$ is that kind which has the highest transition temperature. The result may be displayed as a phase diagram in the $\overline{\Gamma}_1-\overline{\Gamma}_2$ plane at $T=0$ reported in Fig. 6.

Let us first investigate the results of the model for the two extreme concentrations $x=0.05$ and $x=1$. We shall see in the next section that the assumption $\Theta=\Theta^*$ is justified at these two concentrations, so that both Θ and T_N are known from experiment. We also know from neutron experiments that $CeSb_{0.95}Te_{0.05}$ is a type-I antiferromagnet[8] and CeTe a type-II antiferromagnet.[4] From these data, the use of Eqs. (10) and (11) provides the set of values $(\overline{\Gamma}_1,\overline{\Gamma}_2)$ for $x=0.05$ and $x=1$, respectively. The result is reported in Table II. The condition of self-

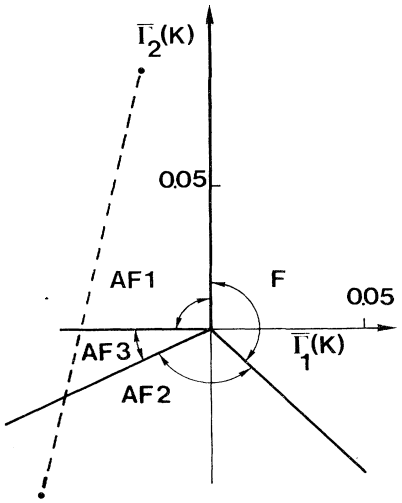

FIG. 6. Magnetic-ordering phase diagram in the $\bar{\Gamma}_1$-$\bar{\Gamma}_2$ plane, where $\bar{\Gamma}_1$ and $\bar{\Gamma}_2$ are the effective exchange integrals between nearest and next-nearest neighbors in the two-parameter Heisenberg model. The dotted line is parametrized by the variations of $\bar{\Gamma}_1(x)$ and $\bar{\Gamma}_2(x)$ in $CeSb_{1-x}Te_x$ reported in Fig. 6 in the whole range $0.05 \leq x \leq 1$.

consistency of the model is that the type of magnetic ordering chosen to calculate $(\bar{\Gamma}_1, \bar{\Gamma}_2)$ from T_N and Θ, by inverting Eqs. (4) and (5), is also the ordering deduced from the set $(\bar{\Gamma}_1, \bar{\Gamma}_2)$ according to the diagram in Fig. 6. It can be checked that this condition is fulfilled in the present case investigated for both $x = 0.05$ and $x = 1$. Hulliger and Ott[11] have studied the exchange interactions in $CeP_{1-x}S_x$ which is a very similar solid solution since we are also in the presence of a mixing between a type-I and a type-II antiferromagnet. These authors have shown that the variations of $\bar{\Gamma}_1$ and $\bar{\Gamma}_2$ was in first approximation a linear function of the sulfur concentration. Let us extend this result to the case of $CeSb_{1-x}Te_x$ by assuming that $\bar{\Gamma}_1(x)$ and $\bar{\Gamma}_2(x)$ are given by a linear interpolation between the sets $(\bar{\Gamma}_1, \bar{\Gamma}_2)$ at $x = 0.05$ and $x = 1$ (Fig. 6). This corresponds to the broken line in the phase diagram of Fig. 6, which predicts that in the range $0.64 < x < 0.79$, the type-III antiferromagnetic ordering is stable. At lower concentrations x we have a type-I antiferromagnet and at $x > 0.79$ the type-II antiferromagnet is stable. From Eq. (7) we can then calculate $T_N(x)$. The result is reported in Fig. 3. The agreement with experiment is reasonably good. The model well accounts for the existence of a minimum in the curve $T_N(x)$. Up to $x \simeq 0.7$ the deviation between theory and experiment is quantitatively small and may be imputed to a small curvature of the curves $\bar{\Gamma}_1(x)$ and $\bar{\Gamma}_2(x)$. The only significant disagreement concerns higher tellurium concentrations, and we shall discuss this point later. It should be noticed, however, that linear variations of $\bar{\Gamma}_1$ and $\bar{\Gamma}_2(x)$, although compatible with nonmonotonic variations of $T_N(x)$, imply linear variations of $\Theta(x)$. We have shown in the preceding section that the curve $\Theta^*(x)$ goes through a deep minimum at $x \simeq 0.5$. Let us assume one moment that $\Theta \sim \Theta^*$ also for this concentration x. In that case we can use Eqs. (4) and (5) to calculate $\bar{\Gamma}_1$ and $\bar{\Gamma}_2$ at $x = 0.5$, following the procedure above mentioned for $x = 0.05$ and $x = 1$. However, the condition of self-consistency on the magnetic ordering in the course of this procedure is not fulfilled for any of the magnetic orderings. It means that the large negative value of Θ at $x \simeq 0.5$ if $\Theta \simeq \Theta^*$ is not compatible with the small Néel temperature in the framework of the two-parameter model. It is the purpose of Sec. II B to investigate the possibility to input the nonlinear behavior of $\Theta^*(x)$ to crystal-field effects.

B. Crystal-field effects

The comparison between $\Theta(x)$ and $\Theta^*(x)$ supposed implicitly that these two quantities are identical. This is true only in the absence of crystal-field effect. When $\Delta \neq 0$, however, the crystal field's only magnetic susceptibility of the $J = \frac{5}{2}$ manifold reads[12]:

$$\frac{C}{\chi} + \Theta = \frac{21T(1+2e^{-\delta})}{5+26e^{-\delta}+(32/\delta)(1-e^{-\delta})}, \qquad \delta = \frac{\Delta}{k_B T} . \tag{7}$$

To simplify the notations, we shall take $k_B = 1$, which amounts to express the energy Δ in kelvins. Equation (7) can be written

$$\chi = \frac{C}{T - \Theta_1(T)} , \tag{8}$$

with

$$\Theta - \Theta_1(T) = \frac{21T(1+2e^{-\delta})}{5+26e^{-\delta}+(32/\delta)(1-e^{-\delta})} - T . \tag{9}$$

At high temperatures where $\delta \ll 1$, a Taylor's expansion as a function of δ can be performed, to give

TABLE II. Typical results of the molecular-field approximation to describe magnetic properties of $CeSb_{1-x}Te_x$. $\bar{\Gamma}_1$ and $\bar{\Gamma}_2$ are effective exchange constants in the two-parameter Heisenberg model. Θ and T_N are the calculated paramagnetic Curie temperature and Néel temperature, respectively. At $x = 0.05$ and $x = 1$, $\bar{\Gamma}_1$ and $\bar{\Gamma}_2$ have been chosen so that the model reproduces exactly the experimental data denoted by an asterisk.

x	Phase	$\bar{\Gamma}_1/k_B$ (10^{-2} K)	$\bar{\Gamma}_2/k_B$ (10^{-2} K)	Θ (K)	T_N (K)
0.05	AF1	−2.3	+9.2	+1.57*	3.75*
0.64	AF1→AF3	−4.35	−0.0512	−3.06	1.01
0.79	AF3→AF2	−4.8	−2.40	−4.20	0.84
1	AF2	−5.6	−5.7	−5.9*	2.00*

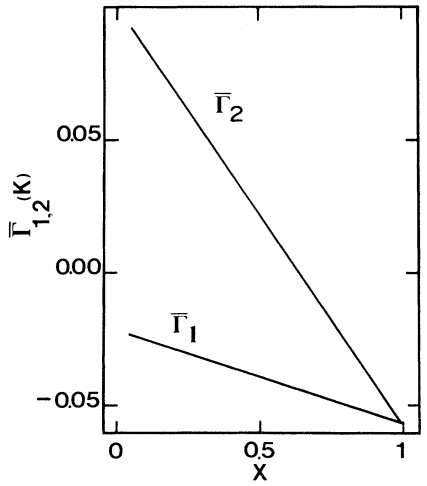

FIG. 7. Theoretical variations of the effective exchange integrals $\bar{\Gamma}_1$ and $\bar{\Gamma}_2$ between nearest and next-nearest neighbors, respectively, as a function of the composition x in the two-parameter Heisenberg model, resulting from a linear interpolation between $x=0.05$ and $x=1$.

$$\Theta-\Theta_1(T)\simeq\frac{8T\delta^2}{189}\ . \tag{10}$$

$\Theta_1(T)$ should not be confused with Θ^* because Θ_1 depends on temperature. According to Eqs. (8) and (10) we can write

$$\chi^{-1}=\frac{1}{C}\left[T-\Theta+\frac{8\Delta^2}{189T}\right]+TO(\delta^2)\ , \tag{11}$$

where $O(\delta^2)$ is the residue of the series development as a function of δ, proportional to δ^3. From Eq. (11) we can derive the two regression coefficients of Eq. (1) in a least-squares fit of the curve $\chi^{-1}(T)$. The first one is the effective Curie constant C^* defined by

$$\frac{C}{C^*}=C\frac{d}{dT}\left[\frac{1}{\chi}\right]=1-\frac{8\Delta^2}{189T^2}\ . \tag{12}$$

Since the least-squares fit is performed in the temperature range $150<T<300$ K, we can take $T=250$ K in Eq. (12). Δ depends on x. The highest value of $|\Delta|$ is found for a typical Te concentration $x=0.5$ where a value $\Delta\simeq-200$ K has been deduced from susceptibility measurements.[13] As usual Δ is defined by $\Delta=E(\Gamma_8)-E(\Gamma_7)$. The negative sign of Δ then means that the ground states belong to the Γ_8 quartet. For $\Delta=-200$ K, $(C^*-C)/C\simeq3\%$. This is the relative error $\Delta C/C$, when C^* is replaced by C as it has been done in Eq. (1). At other concentrations x, $|\Delta|$ and then $\Delta C/C$ will be even smaller, and we can then neglect it. That is the very reason why the effective moment μ could be deduced unambiguously from experiments in Table I. The second regression coefficient is deduced from Eqs. (1), (11), and (12):

$$\Theta^*=\frac{C^*}{C}\left[\Theta-\frac{16\Delta^2}{189T}\right]\ . \tag{13}$$

Replacing C^*/C by 1 in Eq. (13), we get the approximate expression,

$$\Theta^*\simeq\Theta-\frac{16\Delta^2}{189T}\ , \tag{14}$$

valid if $T\gg\Delta$. This correction may be very large. For the same example with $T=250$ K and $\Delta=-200$ K, Eq. (10) gives $\Theta-\Theta^*=13.5$ K for $x\simeq0.5$. In principle when δ is large, the series development in powers of δ is not justified. In such a case the correct procedure is to deduce Θ from the theoretical fit of the experimental curve $\chi(T)$ by Eq. (13). It turns out, however, that the result of this fit reproduces (within 10%) the value of $\Theta-\Theta^*$ as given by Eq. (20). In the first approximation, we have then a fortuitous cancellation of the terms in order higher than δ^2 in the series development of χ as a function of Δ. As a

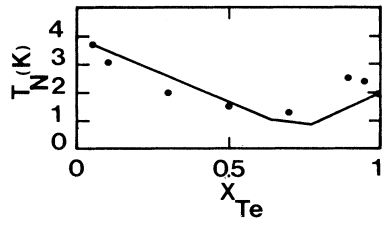

FIG. 8. Theoretical curve of the Néel temperature T_N as a function of x in the two-parameter Heisenberg model. Experimental points are also reported for comparison.

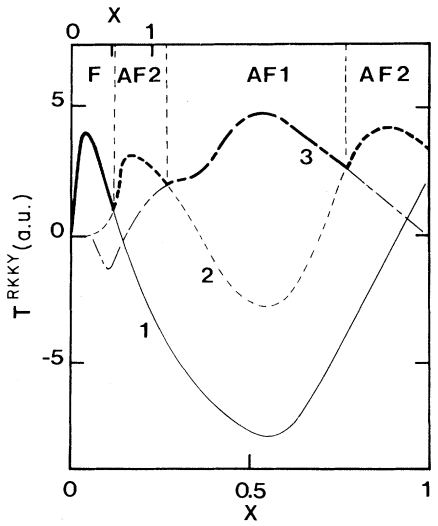

FIG. 9. Temperature $T^{RKKY}(q)$, proportional to the q component of the Fourier transform of the RKKY range function plotted against the composition x, for the two values of the ratio α/d defined in Eq. (18): $\alpha/d=1.5$ (lower scale), and $\alpha/d=0.3$ (upper scale). Calculations have been done for $\vec{q}=(0,0,0)$ (curve 1), $\vec{q}=(\frac{1}{2},\frac{1}{2},\frac{1}{2})$ (curve 2), and $\vec{q}=(1,0,0)$ (curve 3). The magnetic structure, determined by the $\vec{q}$ vector which maximizes $T^{RKKY}(\vec{q})$ is also reported: F is ferromagnetic arrangement, and AF1,2 stand for the antiferromagnetic ordering of the first and second kind. The part of the curves where $T_{RKKY}(\vec{q})$ coincide with the magnetic ordering temperature in the RKKY model are drawn thicker.

consequence, the renormalization of Θ associated with crystal-field effects is contained in the simpler equation (20), for any value of Δ. In particular Eq. (14) accounts for the difference between the experimental value of Θ^* and the theoretical value $\Theta=-2$ K deduced from Eq. (5) with the values of $\bar{\Gamma}_1$ and $\bar{\Gamma}_2$ given in Fig. 7, for $x\sim0.5$. For the two boundary concentrations $x=0.05$ and $x=1$, $|\Delta|<50$ K so that $\Theta-\Theta^*<0.8$ K, which is negligible. This justifies that we have replaced Θ by Θ^* to calculate $\bar{\Gamma}_1$ and $\bar{\Gamma}_2$ according to Eqs. (4) and (5) for $x=0.05$ and $x=1$. From these results, we can suppose that the nonlinear variations of Θ^* as a function of x, with a broad minimum at $x\simeq0.5$, are due to crystal-field effects, and are consistent with a linear decrease of Θ with x in the whole range $0.05<x<1$. To be convincing, however, the argument should lay on an experimental determination of $\Delta\simeq-200$ K at $x=0.5$ independent of the magnetic susceptibility measurements. Neutron experiments and transport measurements are required for this purpose. For the time being, we can only say that the attribution of the minimum of $\Theta^*(x)$ at $x\sim0.5$ to crystal-field effects is a reasonable assumption. In the next paragraph we explore the other alternative, that the minimum is related to a RKKY oscillation.

Another motivation for the study of RKKY interactions comes from the fact that in the range $0.7<x<1$, a maximum of T_N is observed, followed by a decrease of T_N with x up to $x=1$, while our model in Sec. II predicts a monotonous increase of T_N with x in this range of concentrations where the solid solutions are expected to order in the type-II configuration. According to Eq. (4), T_N only depends on $\bar{\Gamma}_2$ with such a spin arrangement, and within our model, a decrease of T_N with x close to $x\simeq1$ would mean an increase of the algebraic value of $\bar{\Gamma}_2$, which supposes a nonmonotonic behavior of $\bar{\Gamma}_2(x)$ going through a minimum at $x\simeq0.9$. We must recall that, by definition, $\bar{\Gamma}_2$ is an effective exchange integral, which is sensitive to the long-range interaction $\Gamma(R_{ij})$. The oscillating behavior of $\bar{\Gamma}_2$ may be result of the RKKY-type oscillations of the indirect exchange $\Gamma(R_{ij})$ via the free carriers at a long-range scale, as a function of x and the carrier concentration.

C. RKKY interactions

By analogy with other semiconducting lanthanide compounds,[14] we could suggest that such variations of Θ^* are the response of the RKKY interaction to the variation of the conduction-electron population in the $5d$ orbital, as x is varied. The paramagnetic Curie temperature derived from the RKKY exchange interaction with the spherical band approximation is[15]

$$\Theta=Ak_F^4\sum_m \mathcal{F}(2k_FR_m)\ . \tag{15}$$

A is a coefficient of proportionality which does not depend on the wave vector at the Fermi energy, k_F. $\mathcal{F}$ is the RKKY function,

$$\mathcal{F}(2k_FR_m)=\frac{2k_FR_m\cos(2k_FR_m)-\sin(2k_FR_m)}{(2k_FR_m)^4}\ . \tag{16}$$

In first approximation, we can presume that the number of conduction electrons per magnetic ion, n, is proportional to x:

$$n=\alpha x \tag{17}$$

It follows that k_F is related to x according to the law,

$$k_F=\left[\frac{\alpha}{d}\right]^{1/3}2\pi\left[\frac{3x}{16\pi}\right]^{1/3}\ . \tag{18}$$

d is the degeneracy of the conduction band. The factor $(\alpha/d)^{1/3}$ then appears as a scaling parameter of the abscissa in the curve $\Theta(x)$, while A is a scaling coefficient for the y axis. We do indeed find a good agreement between the experimental values of $\Theta^*(x)$ and the theoretical expression in Eq. (15) at all tellurium concentrations for

$$\frac{\alpha}{d}=1.5\ . \tag{19}$$

This is illustrated in Fig. 8. In particular a sharp maximum at $x=0.04$ is predicted, which agrees with the large value of Θ^* observed at $x=0.02$.

Just as in the two-parameter model, we can derive the ordering temperature from the Fourier transform of the RKKY range function[16]:

$$T_{C,N}=T^{\mathrm{RKKY}}(\vec{q}=\vec{k})\ ,$$

$$T^{\mathrm{RKKY}}(\vec{q})=Ak_F^4\sum_m e^{i\vec{q}\cdot\vec{R}_m}\mathcal{F}(2k_FR_m)\ , \tag{20}$$

where $\vec{k}$ is the wave vector of the magnetic structure, i.e., the vector $\vec{q}$ which maximizes $T^{\mathrm{RKKY}}(\vec{q})$ in Eq. (20). With the RKKY interaction, the phase AF3 is not stable and the wave vectors of interest to make contact with the previous two-parameter Heisenberg model are $q=(0,0,0)$, $q=(1,0,0)$, and $q=(\frac{1}{2},\frac{1}{2},\frac{1}{2})$. The temperature $T^{\mathrm{RKKY}}(\vec{q})$ has been calculated as a function of k_F for such values of q in the fcc lattice.[17] This result is illustrated in Fig. 9 where we have plotted $T^{\mathrm{RKKY}}(\vec{q})$ as a function of x, according to Eqs. (18) and (19). At low concentration x the maximum value of $T^{\mathrm{RKKY}}(\vec{q})$ is obtained for $q=k=0$ so that the ferromagnetic phase is stabilized. Then the AF2 phase is stable up to $x=0.3$. These results are obviously in complete disagreement with experiments since CeSb is not ferromagnetic in the absence of external field and that $CeSb_{1-x}Te_x$ for $x=0.05$ is a type-I antiferromagnet. According to the model, however, this phase AF1 is found to be stable for $x>0.3$, up to $x=0.8$, and in the range $0.8<x<1$, the model predicts the AF2 spin arrangement, in agreement with experiments. Moreover, the maximum of the curve $T_N(x)$ at $x=0.9$, and the decrease of T_N with x for the AF2 phase in the range $0.9<x<1$ are also accounted for by the model. The main disagreement between theory and experiments for $x>0.3$ is that the model, according to Fig. 9 predicts a maximum of $T_N(x)$ at $x\simeq0.6$, instead of a minimum. This is connected with the incompatibility between large negative values of Θ and the small values of T_N, a result which we had already inferred in the two-parameter model. We can then conclude that the agree-

ment between the RKKY model and experiment improves as x increases: For $x<0.3$ the model fails to reproduce the spin arrangement in the ordered phase and the evolution of T_N as a function of x. In the range $0.3<x<0.8$ the model still fails to give the proper variations of $T_N(x)$ but accounts for the nature of magnetic ordering. At $x>0.8$, an overall agreement between theory and experiments is obtained. This behavior can be understood as follows. In the AF2 structure of a fcc lattice, nearest-neighbor interactions always cancel. This is manifested in the fact that T_N only depends on $\overline{\Gamma}_2$ in Eq. (4). It follows that this structure is imposed by long-range magnetic interactions like the RKKY interaction, and is not sensitive to short-range superexchange interactions, so that the model may fit the magnetic properties of $CeSb_{1-x}Te_x$ at $x>0.8$. At smaller concentrations, however, the AF2 structure is no longer stable and the nearest-neighbor interactions become of a primary importance. We can then expect the magnetic properties of the solutions to be dominated by short-range interactions, which is the reason for the failure of the RKKY model, and also the reason for the success of the two-parameter model to account for the variations of $T_N(x)$. Since $T^{\mathrm{RKKY}}[q=(\frac{1}{2},\frac{1}{2},\frac{1}{2})]$ almost vanishes for $x<0.1$ in Fig. 9, the experimental variations of $T_N(x)$ at such concentrations are by no means connected with the RKKY interactions. Moreover, the large value of α/d is rather unphysical and makes the interpretation of the curve $\Theta(x)$ in terms of RKKY interaction unlikely. In effect α is not expected to be significantly different from unity except in the limit of small x, because CeSb is a n-type material with a carrier-concentration $n\simeq 10^{19}$ cm^{-3} according to transport experiments.[3] Owing to the threefold degeneracy of the t_{2g} branch of the $5d$ conduction band in NaCl compounds, we have $d=3$, so that we expected a typical ratio $\alpha/d\simeq\frac{1}{3}$ smaller than unity, at variance with the value in Eq. (19). Then we regard the overall agreement between the experimental variations of $\Theta^*(x)$ and the curve $\Theta(x)$ deduced from Eq. (15) as accidental.

The results obtained for $\alpha/d=\frac{1}{3}$ are readily seen in Fig. 9, since this choice of α/d only contracts the abcissa by a factor 4.5 with respect to the case $\alpha=1.5$. In the range $0.1<x<1$, the variation of $\Theta(x)$ thus obtained (curve 1 in Fig. 9) decreases monotonically with x, in agreement with the prediction of the two-parameter model described in the previous paragraph. Also the AF2 phase now extends in the whole range $0.5<x<1$. In this range, T_N goes through a maximum in agreement with experiments. This corroborates that RKKY interactions well account for the magnetic properties of $CeSb_{1-x}Te_x$ in the AF2 phase at high tellurium concentrations, typically $x>0.7$. At lower concentrations, however, the same disagreement between theory and experiments are observed as in the case $\alpha/d=1.5$ and the model predicts a stable ferromagnetic ordering extending in the whole range $0<x<0.5$.

D. Limits of the isotropic models

The above studies give an overall understanding of the magnetic properties of $CeSb_{1-x}Te_x$ in the whole range $0.05<x<1$, in the framework of the two-parameter Heisenberg model, with an extra RKKY oscillation of $T_N(x)$ in the range $0.7<x<1$. It must be noticed however, that the nonlinear variation of Θ^* was deduced from the nonlinear variation of Δ with x. The problem now is to understand why the variations of Δ are not linear.

Also the two-parameter model is purely phenomenologic, and does not tell anything on the physical nature of the magnetic interactions from which $\overline{\Gamma}_1$ and $\overline{\Gamma}_2$ are issuing. With this respect, we have shown that at $x<0.05$ isotropic interactions do not dominate the magnetic behavior of the material. In fact the orbital momentum of the Ce^{3+} ion is large ($l=3$), so that the spin-orbit coupling is strong and the interactions are strongly anisotropic in nature. It is the purpose of the next section to study such anisotropic interactions, together with their ability to describe magnetic properties at $x<0.05$ and nonlinear variations of Δ with x, which are beyond the scope of the above models.

IV. ANISOTROPIC EXCHANGE MODELS

Mainly two models compete for the calculation of the magnetic exchange interactions in CeSb and other cerium compounds, namely the model of Kasuya *et al.*[18] and that of Cooper *et al.*[19] This last model follows the theory for two-ion anisotropic exchange of Coqblin and Schrieffer.[20]

Both models lay on the same physical basis: the indirect spin-spin interaction mediated via charge carriers originates from the hybridization between localized $4f$-electron and charge-carrier states. We use the terminology "charge" carriers rather than "free" carriers to denote conduction electrons, or holes in the valence band, for reasons which will be explicated later. The reason why the hybrid exchange interaction dominates other anisotropic indirect-exchange channels is that the $4f$ level is located close to the conduction- and valence-band states in cerium, contrary to the situation met in other rare earths. This interaction is strongly anisotropic due to the large spin-orbit coupling of the intermediate states, associated to the finite value of the orbital angular momentum $l=3$ of the Ce^{3+} ion.[20,21]

The main difference between the two models above mentioned concerns the description of the charge carriers in spin-orbit coupled states. One approach consists in the tight-binding description of the Bloch wave function:

$$\Psi_{kjM}(\vec{r})=\sum_n e^{i\vec{k}\cdot\vec{R}_n}\psi_{lsjM}(\vec{r}-\vec{R}_n)\,, \tag{21}$$

where the suffix n labels the sites of the Ce ions. The Wannier function ψ_{lsjM} is a linear combination of atomic orbitals (LCAO) which have the orbital angular momentum l, spin s, and a total angular momentum state $|j,M\rangle$. Kasuya *et al.* have considered the atomic limit which consists in replacing Ψ_{kjM} by its limit at $k=0$:

$$\Psi_{kjM}(\vec{r})=\sum_n \psi_{lsjM}(\vec{r}-\vec{R}_n)\,. \tag{22}$$

With this regard the charge carrier is not free, but is localized in atomic orbitals around each site.

However, the materials we are dealing with are semiconductors and metals, so that the Bloch sites with the electrons traveling rapidly through the whole crystal is a more appropriate description of the charge carriers. Coqblin and Schrieffer have considered the free-electron limit, in which Eq. (21) is replaced by

$$\Psi_k(\vec{r}) \propto e^{i\vec{k}\cdot\vec{r}}\sigma \ , \tag{23}$$

where σ is the spinor for the spin $s=\frac{1}{2}$. Then the free-carrier behavior is considered from the point of view of scattering of spherical place waves, according to the standard decomposition

$$e^{i\vec{k}\cdot\vec{r}}=\sum_{l,m}(2l+1)i^l j_l(kr)e^{ikr}Y_l^m(\theta_k,\phi_k) \ , \tag{24}$$

where j_l are Bessel functions and Y_l^m the spherical harmonics.

To investigate more quantitatively the magnetic properties associated with such wave functions, it is necessary to specify the Hamiltonian. The Coqblin-Schrieffer theory is based on the Anderson Hamiltonian,[22]

$$\begin{aligned} H &= H_0+H_1 \ , \\ H_0 &= \sum_{k,M}\epsilon_k n_{kM}+\sum_M E_0 n_M+\frac{U}{2}\sum_{M,M'} n_M n_{M'} \ , \\ H_1 &= \sum_{k,M} V_k c_{k,M}^{\dagger}c_M+V_k^{*}c_M^{\dagger}c_{k,M} \ . \end{aligned} \tag{25}$$

H_0 includes, respectively, single electron band, the $4f^1$ configuration energy, and a Coulomb energy to take into account correlation effects when an electron is added to the $4f^1$ configuration. $c_M^{\dagger}$ creates an electron in the state $j=\frac{5}{2}$ and z projection M. $c_{kM}^{\dagger}$ creates a free carrier with wave vector $\vec{k}$ in the quantum state $|j=\frac{5}{2},M\rangle$.

The hybridization energy H_1 is considered as the perturbation term, which is the usual procedure of the Schrieffer-Wolff transformation.[23] The idea of the Schrieffer-Wolff transformation is to perform successive canonical transformations aimed at eliminating odd powers of the mixing parameter V_k. The transformed Hamiltonian is

$$\tilde{H}=\cdots e^{S^{(3)}}e^{S^{(1)}}He^{-S^{(1)}}e^{-S^{(3)}}\cdots \ , \tag{26}$$

where the superscript on the S matrix indicates the order in V_k of each successive term. S^k is chosen so that the transformed Hamiltonian is

$$\tilde{H}=H_0+H^{(2)}+H^{(4)}+\cdots \ , \tag{27}$$

where the superscript on H indicates the order in V_k of each successive term. Coqblin and Schrieffer have calculated the term in $H^{(2)}$ associated with the Kondo-type coupling of localized f electrons to free carriers but neglected $H^{(4)}$. Actually the total effective interaction between localized moments is then

$$\langle i|H_{\text{eff}}|f\rangle=\langle i|H^{(4)}|f\rangle+\sum_{\alpha}\frac{\langle i|H^{(2)}|\alpha\rangle\langle\alpha|H^{(2)}|f\rangle}{E_0-E_\alpha} \ , \tag{28}$$

where $|i\rangle$ and $|f\rangle$ are degenerate ground states of H_0; E_α represents the energy of the intermediate states. H_{eff} is fourth order in V_k and higher-order terms have been neglected. From Eq. (28) we can derive the interaction between a pair of Ce^{3+} ions separated by R_{ij} as follows:

$$\sum_{M,M'}\Gamma^{M,M'}(R_{ij})\left[c_{M'}^{\dagger}(i)c_M(i)-\sum_{M''}\langle n_{M''}(i)\rangle\right]\times\left[c_M^{\dagger}(j)c_{M'}(j)-\sum_{M''}\langle n_{M''}(j)\rangle\right] \ , \tag{29}$$

which defines the coupling constant $\Gamma^{M,M'}(R_{ij})$. The anisotropic nature of this interaction lies in the fact that $\Gamma^{MM'}$ depends on M and M', contrary to the quantity Γ in Eq. (2). To facilitate the discussion, it is convenient to sort out the dependence and write

$$\Gamma^{M,M'}(R_{ij})=F(R_{ij})G(M,M') \ , \tag{30}$$

where $F(R_{ij})$ is the range function. To calculate this expression, however, is a difficult task and further approximations are needed for practical purposes. Cooper *et al.* only considered the contribution to $\Gamma^{MM'}(R_{ij})$ arising from the Coqblin-Schrieffer interaction, so that they dropped the first term in Eq. (28). To the contrary, in a different context, Goncalves da Silva and Falicov[24] have calculated the first term of Eq. (28) in a fourth-order perturbation theory, but dropped the second term. Actually, it is important to build a model which takes into account both terms in Eq. (28), because they both have the same order of magnitude. In this context, an improvement to the Cooper model consists in neglecting the effect of the first term in Eq. (28) on $G(M,M')$ and consider only its effect on the range function $F(R_{ij})$. This is justified because $G(M,M')$ only describes the anisotropy of the spin-spin interactions between $4f$ electrons, which is essentially determined by the symmetry of the $j=\frac{5}{2}$ configuration. This model amounts to simplify the structure of the localized orbitals to include only spin degeneracy in the derivation of $F(R_{ij})$. Such a calculation has been carried out by Proetto and Lopez.[25] The result is

$$F(R_{ij})=\sum_q\frac{|V_q|^2}{N}e^{i\vec{q}\cdot\vec{R}}\sum_k|V_k|^2\frac{(1-f_k)}{(E_0-E_k)^2}\times\left[\frac{f_{k+q}}{\epsilon_{k+q}-\epsilon_q}+\frac{1-f_{k+q}}{\epsilon_{k+q}-E_0}\right] \ . \tag{31}$$

f_k is the occupation number given by the Fermi function. $F(R_{ij})$ can be calculated in the case of a parabolic band $\epsilon_k=\hbar^2k^2/(2m^*)$, assuming that V_q does not depend on q. The first term in the large parentheses contains contributions from both $H^{(2)}$ and $H^{(4)}$. When $|\vec{k}|=|\vec{k}+\vec{q}|=k_F$, the numerator remains finite, but the denominator vanishes, giving rise to a singularity of the Friedel type, and consequently RKKY oscillations which dominate the behavior of $F(R_{ij})$ at large distances. In particular, in the limit $k_FR_{ij}\gg1$, $F(R_{ij})$ reduces to

$$F(R_{ij})=k_F^4\mathcal{F}(2k_FR_{ij}) \ . \tag{32}$$

The second term in the large parentheses contains contributions from $H^{(4)}$ only, and is then missing in the model of Cooper *et al.* The energy denominator contains E_0 and never vanishes, so that this term does not give an oscillatory behavior, but is always antiferromagnetic with an exponentially decaying strength. In particular, in the limit $k_F R_{ij} \ll 1$, this term is predominant and gives[24,26]

$$F(R_{ij}) \propto -\frac{e^{-2k_0 R}}{k_0^2 R^2} , \tag{33}$$

with k_0 defined by

$$k_0 = \frac{(2m^* E_0)^{1/2}}{\hbar} . \tag{34}$$

V. DISCUSSION

A. Range-function effects

Equation (33) gives at least a partial explanation why RKKY interactions are not sufficient to describe the magnetic properties of $CeSb_{1-x}Te_x$. Villain *et al.*[27] have studied the exchange interactions between different layers in the Ising model. They have been able to fit the zero-temperature phase diagram of CeSb as a function of the applied magnetic field, by a RKKY interaction except for nearest neighbors. Moreover, these authors have shown that the interaction between nonmagnetic layers resulting from the superposition of the RKKY interaction plus an antiferromagnetic interaction decaying exponentially with distance, is sufficient to account for most of the ferro-paramagnetic phases observed in CeSb between 9 and 15 K. Although the authors considered such a short-range interaction as a consequence of a coupling to longitudinal-optic modes, we can also presume that it is simply the superexchangelike term given by Eq. (33). Contrary to Villain *et al.*, Cooper *et al.* did not calculate explicitly $F(R_{ij})$. In fact they used a two-parameter approximation, very similar to the one we used in the previous section, since they truncated $F(R_{ij})$ to the next-nearest neighbors r_2. They only considered $\bar{F}(r_1)$ and $\bar{F}(r_2)$ (or $\bar{\Gamma}_1$ and $\bar{\Gamma}_2$) in Eq. (30), as adjustable parameters which can be chosen in order to fit experimental data. This may be the reason why this model is so successful to describe the magnetic phase diagram of CeBi and CeSb. The advantage of Cooper *et al.* is that the anisotropy does not follow from the arbitrary assumption that the intralayer interaction is large with respect to the interlayer interaction, but is contained in the term $G(M,M')$ which has been calculated explicitly. At this stage, we cannot make any comparison with the model of Kasuya *et al.* because these authors did not calculate the magnetic phase diagram, nor the indirect spin-spin interactions which are fourth order in the mixing potential. They only evaluated second-order effects in the anisotropic mixing p-f integrals and showed that this anisotropy accounted for the $\langle 100 \rangle$ easy axis of magnetization in CeSb,[18] a result which is also inferred from the model of Cooper *et al.*,[19] with the Coqblin-Schrieffer interaction.

B. Anisotropic effects

Up to now we have focused attention to the range function $F(R_{ij})$. However, the anisotropic term $G(M,M')$ is also of fundamental interest. To calculate this quantity, we can notice that the expansion in spherical plane waves in Eq. (24) corresponds to a decomposition of the propagating wave along the basis $|klm\sigma\rangle$ where m and σ are z components of the orbital momentum l and spin $s=\frac{1}{2}$, respectively. The Coqblin-Schrieffer interaction (and the model of Cooper *et al.*) selects out only the f resonant scattering so that only the component $l=3$ in Eq. (24) is considered. This state must be expressed in the $|kM\rangle$ basis, in which the Hamiltonian in Eq. (25) is expressed, with $j=\frac{5}{2}$; we can write

$$|kM\rangle = \alpha_M |k,3,M+\tfrac{1}{2},-\tfrac{1}{2}\rangle + \beta_M |k,3,M-\tfrac{1}{2},+\tfrac{1}{2}\rangle , \tag{35}$$

where α_M and β_M are appropriate Clebsch-Gordan coefficients. It follows that only the $m = M \pm \frac{1}{2}$ components enter the equations, and $G(M,M')$ is proportional to[19]

$$\int_{-1}^{+1} e^{ikRx} |P_{l=3}^{M\pm 1/2}|^2 dx , \tag{36}$$

where $P_l^{M\pm 1/2}$ is the Legendre polynomial. To lowest order in $1/kR$ the only nonvanishing integrals in Eq. (36) are for $M=\pm\frac{1}{2}$. So, the exchange interaction in the model of Cooper *et al.* couples the f-orbital states with $M=\pm\frac{1}{2}$. These states correspond to the f orbitals with $m=0$, i.e., those that pile up charge along the bonding axis between Ce ions. This exchange interaction, however, does not interact with the f-orbital states with $M=\pm\frac{3}{2}$ and $M=\pm\frac{5}{2}$ separately, since the integral in Eq. (36) vanishes for such values of M. It means that the exchange will interact with the two bonding states which are the appropriate mixture of $M=\pm\frac{3}{2}$ and $M=\pm\frac{5}{2}$ states piling the charge along the bonding axis, so as to reproduce the charge symmetry of the $m=0$ states, but will not interact with the two antibonding states piling up the charge outside the bonding axis. The physical meaning of this result is obvious: The exchange interaction between Ce ions breaks the sphericals symmetry of the single isolate Ce^{3+} ion and reduces the symmetry to that of the cubic lattice. Then it contributes to the crystal-field energy. In the presence of the crystal field, the eigenstates of the $4f$ electrons are linear combinations of the functions with different M values and are given by[28]

$$\begin{aligned} \Gamma_7: \quad & |j_z = \mp 0.83\rangle = 0.4083 |\pm\tfrac{5}{2}\rangle - 0.9129 |\mp\tfrac{3}{2}\rangle , \\ \Gamma_8: \quad & |j_z = \pm 1.83\rangle = 0.9129 |\pm\tfrac{5}{2}\rangle + 0.4083 |\mp\tfrac{3}{2}\rangle , \\ & |j_3 = \pm 0.5\rangle = |\pm\tfrac{1}{2}\rangle . \end{aligned} \tag{37}$$

The Γ_7 eigenstates are the antibonding states. $|j_z = \pm 1.83\rangle$ are the bonding states, as well as the two states $|M\pm\frac{1}{2}\rangle$ which are still eigenstates because they have zero-orbital-momentum projection m. These symmetry arguments show that the interaction affects differently the Γ_8 quartet and the Γ_7 doublet, and then affects Δ. This result was inferred in the model of Kasuya

et al.[29] and the same holds true in the model of Cooper *et al.* To make contact with Ref. 25, we will assume that the exchange interaction mostly affects the Γ_8 states.

C. Crystal-field effects

The exchange interaction is responsible for a shift of the Γ_8 level and then a change of the energy Δ, which can be derived from the second-order perturbation theory under the form

$$U=\sum_{i=1}^{2}\sum_{k,M}\frac{|\langle kM|v_k^i|\psi_f\rangle|^2}{E_0-\epsilon_k^i}f_k^i \ . \tag{38}$$

ψ_f is the eigenstate of the Γ_8 quartet; $i=1,2$ specifies the nature of the free carrier and refers to an electron in the conduction band and a hole in the valence band, respectively. v_k^i is the appropriate coupling potential. Equation (38) is the generalization of the expression of U as derived by Kasuya *et al.*[29] Since $E_0<\epsilon_k^i$, U is negative and shifts the Γ_8 level to lower energies, which accounts for the low value of Δ in CeSb and CeBi with respect to the value deduced from the point charge model. It also accounts for the lower value of Δ in CeBi than in CeSb because more free carriers (electrons plus holes) are expected in CeBi due to a significant overlap of the conduction and valence bands, and U is proportional to the carrier concentrations n_i owing to the occupation number f_k^i in Eq. (38). The evolution of Δ as a function of x in $CeSb_{1-x}Te_x$ is even more interesting since Δ goes through a maximum at $x=0.04\pm0.01$. Our model can account for this result if we admit, as Kasuya *et al.* did, that CeSb is a semimetal with a small overlap of conduction and valence bands. When x increases from $x=0$ we expect the hole concentration n_2 in the valence band to decrease and the electron concentration n_1 to increase. These two effects give opposite contributions to Δ. If the *p-f* coupling is stronger than the *d-f* one, the larger contribution to Δ comes from the decrease of the hole concentration, so that Δ increases until the concentration x_m is reached where the valence band is fulfilled. A further increase of x only increases n_1, implying a decrease of Δ. To the contrary, the model of Kasuya *et al.*, which considers the *p-f* mixing alone, cannot account for the peak of $\Delta(x)$ at x_m, but can only account for the increase of $\Delta(x)$ at $x<x_m$.

The reason for this advantage of our model is that it does not depend on the nature of the free carrier, and is the same whether the free carrier originates from *d* electrons on a cerium site or from *p* electrons on an anion site, or from both of them. This property is the consequence of the reduction of the wave function to a plane wave in Eq. (23). In the model of Kasuya *et al.* the wave function is described in terms of the Wannier function in Eq. (22) which depends on the nature of the charge carrier: if $l=1$, Eq. (22) represents an eigenstate of the Γ_{15} point of the Brillouin zone and is then associated with a hole in the valence band. Then this choice of l in the model of Kasuya *et al.* is a reduction of the problem to a nonresonant scattering of carriers of a given type (holes), although the choice $l=3$ in Eq. (24) of the model of Cooper *et al.* is only the approximation of a resonant scattering of free carriers of any type. We used the band-structure terminology in Sec. II, and pointed out that Eq. (22) is an LCAO approach. In the same way Eq. (24) is the decomposition characteristics of muffin-tin theories. The difference is that the wave function in Eq. (23) is assumed to be a plane wave even at the Ce sites. A better approximation would consist in identifying $\Psi_k(\vec{r})$ to a plane wave outside the muffin tin at $r>R$, and to a LCAO inside the muffin tin $r<R$, where R is the radius of the Ce ion. This is the augmented—plane-wave picture (APW), which shows that the reality is somewhere in between the description of the charge-carrier eigenstates by Kasuya and Cooper, respectively.

D. Magnetic properties at $x<0.05$

The fact that the exchange interaction comes from orbital states that pile up the charge along the bonding axis gives strongest coupling in the $\langle 100\rangle$ planes.[15] This coupling is ferromagnetic, which explains the positive value of Θ observed at low concentrations x in $CeSb_{1-x}Te_x$. Nevertheless, the model of Cooper *et al.* does not account for the antiferromagnet ordering between the $\langle 100\rangle$ layers since it favors the ferromagnetic ordering. The antiferromagnetism may be induced by the short-range interactions coming from $H^{(4)}$ [see Eq. (33) and the discussion in Sec. V A]. We have pointed out that one goes from this short-range interaction to the RKKY long-range interaction as the free-carrier concentration n increases. So the increase of x from $x=0$ will reduce the short-range antiferromagnetic interaction, which implies a decrease of T_N and an increase of Θ, in agreement with experiments. Then at $x\simeq0.02$ the range function $F(R_{ij})$ oscillates with R_{ij}, and so does the Fourier transform $F(q=0)$ as a function of n or x, but the oscillations as deduced from Eq. (31) are quantitatively different from the RKKY ones.[25] Since $\Theta\propto F(q=0)$ the maximum of Θ at $x\simeq0.02$ may be due to such an oscillation, shifted with respect to the RKKY predictions. This shift shows itself in the anomalous ratio α/d in Eq. (19) when we try to fit experiments with the RKKY model. At larger concentrations $x\gg0.02$, however, the limit in Eq. (32) is reached for smaller values of R_{ij} and the RKKY model should provide a good description of the variations $\Theta(x)$ because Θ is essentially sensitive to the long-range part of the interactions. To the contrary $T_N\propto F(q=Q)$ where Q is the wave vector of the magnetic order. Since Q is large, T_N is mainly sensitive to the range function $F(R_{ij})$ at small distances R_{ij}, where the antiferromagnetic interactions create the deviation from the RKKY function. This explains why $T_N(x)$ cannot be deduced from the RKKY model which, however, provides a good description of the curve $\Theta(x)$ for $x>0.05$, a result which we had noticed in Sec. II.

VI. CONCLUSION

Magnetic properties of $CeSb_{1-x}Te_x$ solid solution have been investigated. To account for the experimental results, we have studied the properties of the fourth-order indirect exchange Hamiltonian in the mixing parameter, derived after a canonical transformation of the Schrieffer-Wolff type is applied to the Anderson model.

This indirect magnetic interaction H_{eff} contains the magnetic exchange derived by Cooper *et al.*, originating from the two-ion anisotropic exchange of Coqblin and Schrieffer, but also contains antiferromagnetic short-range interactions which were not present in the models of Refs. 19 and 20. Even so, H_{eff} is not the only exchange mechanism which may occur in these materials. In particular this model only considers a resonant exchange between free carriers (electrons or holes) and the $4f$ electrons. Nonresonant processes also exist. For example, we have shown that the exchange interaction of Kasuya *et al.* has the same symmetry and the same fundamental properties than the interaction of Cooper *et al.*, with the limitation that the model of Kasuya *et al.* only considers the mixing of holes in the valence band with the $4f$ electrons on the Ce sites. The problem on a theoretical point of view, is not to build an untractable model which would take into account all the possible magnetic interactions, but to select exchange processes which dominate the physical properties of the material. In this respect, we can conclude that H_{eff} is the simplest Hamiltonian which satisfies this purpose at least qualitatively.

---

*On leave from Laboratoire de Physique des Solides, CNRS, 1 place A. Briand, 92190 Meudon, France.

[1]J. Rossat-Mignod, P. Burlet, J. Villain, H. Bartholin, W. Tcheng Si, D. Florence, and O. Vogt, Phys. Rev. B 16, 440 (1977); P. Fischer, B. Lebech, G. Meier, B. D. Rainford, and O. Vogt, J. Phys. C 11, 345 (1978); G. Meier and P. Fischer, *ibid.* 11, 1973 (1978).

[2]R. J. Birgeneau, E. Bucher, J. P. Maita, L. Passeil, and K. C. Turberfield, Phys. Rev. B 8, 5345 (1973).

[3]M. Escorne, A. Mauger, D. Ravot, and J. C. Achard, J. Phys. C 14, 1821 (1981).

[4]H. R. Ott, J. K. Kjems, and F. Hulliger, Phys. Rev. Lett. 42, 1378 (1979).

[5]F. Hulliger, B. Natterer, and H. R. Ott, J. Magn. Magn. Mater. 8, 87 (1978).

[6]M. Escorne, D. Ravot, J. C. Achard, and A. Mauger, J. Appl. Phys. 53, 2061 (1982).

[7]D. Ravot, J. C. Achard, and J. Rossat-Mignot, *The Rare Earth in Modern Science and Technology,* edited by G. J. Mac Carthy, H. B. Silber, and J. J. Rhyne (Plenum, New York, 1982), p. 445.

[8]P. Burlet, S. Kuezel, J. M. Effantin, J. Rossat-Mignod, D. Ravot, and H. Bartholin, in The 7th International Conference on Solid Compounds of Transition Elements, Grenoble, 1982 (unpublished).

[9]W. Zinn, J. Magn. Magn. Mater. 3, 23 (1976).

[10]J. S. Smart, *Effective Field Theories of Magnetism* (Saunders, Philadelphia, 1966), p. 58.

[11]F. Hullinger and H. R. Ott, J. Phys. (Paris) Colloq. C-5, 128 (1979).

[12]E. D. Jones, Phys. Lett. 22, 266 (1966).

[13]D. Ravot, thèse de doctorat d'état, Paris, 1983 (unpublished).

[14]F. Holtzberg, T. R. Mac Guire, S. Methfessel, and J. C. Suits, Phys. Rev. Lett. 13, 18 (1964).

[15]P. G. De Gennes, J. Phys. Radium 23, 630 (1962).

[16]J. Villain, J. Phys. Chem. Solids 11, 303 (1959).

[17]J. Sakurai, Y. Kubo, T. Kondo, J. Pierre, and E. F. Bertaut, J. Phys. Chem. Solids 34, 1305 (1973).

[18]K. Takegahara, H. Takahashi, A. Yanase, and T. Kasuya, J. Phys. C 14, 737 (1981); T. Kasuya, *Electron Correlations and Magnetism in Narrow Band Systems,* edited by T. Moriya (Springer, Berlin, 1981), p. 237; K. Takagahara, A. Yanase, and T. Kasuya, J. Phys. (Paris) Colloq. C-5, 327 (1980), and erratum; J. Phys. (Paris) 41, 1231 (1980).

[19]R. Siemann and B. R. Cooper, Phys. Rev. Lett. 44, 1015 (1980); B. R. Cooper and R. Siemann, *Crystalline Electric Field and Structural Effects in f-electron Systems,* edited by J. E. Crow, R. P. Guertin, and T. W. Mihalisin (Plenum, New York, 1980), p. 241; B. R. Cooper, J. Magn. Magn. Mater. 29, 230 (1982).

[20]B. Coqblin and J. R. Schrieffer, Phys. Rev. 185, 847 (1969).

[21]P. M. Levy, Solid State Commun. 7, 1813 (1969).

[22]P. W. Anderson, Phys. Rev. 124, 41 (1961).

[23]J. R. Schrieffer and P. A. Wolff, Phys. Rev. 149, 491 (1966).

[24]C. E. T. Goncalves da Silva and L. M. Falicov, J. Phys. C 5, 63 (1972).

[25]C. Proetto and A. Lopez, Phys. Rev. B 24, 3031 (1981); *Valence Instabilities,* edited by P. Wachter and H. Boppart (North-Holland, Amsterdam, 1982), p. 555.

[26]P. W. Anderson, Phys. Rev. 79, 350 (1950).

[27]J. Villain, M. B. Gordon, and J. Rossat-Mignod, Physica 102B, 2621 (1980).

[28]Y. Ebina and N. Tsuya (unpublished).

[29]H. Takahashi, K. Takegahara, A. Yanase, and T. Kasuya, *Valence Instabilities,* edited by P. Wachter and H. Boppart (North-Holland, Amsterdam, 1982), p. 379; K. Takegahara, H. Takahashi, A. Yanase, and T. Kasuya, Solid State Commun. 39, 857 (1981).